Research Article

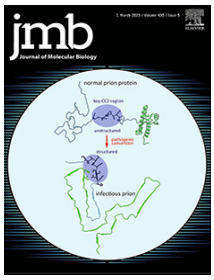

Multi-level Force-dependent Allosteric Enhancement of αE-catenin Binding to F-actin by Vinculin

Nicolas A. Bax [a†], Amy Wang [a,b†], Derek L. Huang [c], Sabine Pokutta [a], William I. Weis [a*] and Alexander R. Dunn [b,d*]

***a* - Departments of Structural Biology and Molecular & Cellular Physiology,** *Stanford University School of Medicine, United States*

***b* - Department of Chemical Engineering,** *Stanford University School of Engineering, United States*

***c* - Graduate Program in Biophysics,** *Stanford University, United States*

***d* - Stanford Cardiovascular Institute,** *Stanford School of Medicine*

Correspondence to William I. Weis and Alexander R. Dunn: *bill.weis@stanford.edu (W.I. Weis), alex.dunn@stanford.edu (A.R. Dunn) @bax1337 (N.A. Bax), @amywang01 (A. Wang), @Dunn_Lab (A.R. Dunn)*

https://doi.org/10.1016/j.jmb.2023.167969

Edited by James Sellers

Abstract

Classical cadherins are transmembrane proteins whose extracellular domains link neighboring cells, and whose intracellular domains connect to the actin cytoskeleton via β-catenin and α-catenin. The cadherin-catenin complex transmits forces that drive tissue morphogenesis and wound healing. In addition, tension-dependent changes in αE-catenin conformation enables it to recruit the actin-binding protein vinculin to cell–cell junctions, which contributes to junctional strengthening. How and whether multiple cadherin-complexes cooperate to reinforce cell–cell junctions in response to load remains poorly understood. Here, we used single-molecule optical trap measurements to examine how multiple cadherin-catenin complexes interact with F-actin under load, and how this interaction is influenced by the presence of vinculin. We show that force oriented toward the (−) end of the actin filament results in mean lifetimes 3-fold longer than when force was applied towards the barbed (+) end. We also measured force-dependent actin binding by a quaternary complex comprising the cadherin-catenin complex and the vinculin head region, which cannot itself bind actin. Binding lifetimes of this quaternary complex increased as additional complexes bound F-actin, but only when load was oriented toward the (−) end. In contrast, the cadherin-catenin complex alone did not show this form of cooperativity. These findings reveal multi-level, force-dependent regulation that enhances the strength of the association of multiple cadherin/catenin complexes with F-actin, conferring positive feedback that may strengthen the junction and polarize F-actin to facilitate the emergence of higher-order cytoskeletal organization.

Introduction

Classical cadherins are transmembrane proteins that mediate homophilic interactions between cells, and are fundamental to the construction of animal tissues.[1–2] Cadherins are linked to the underlying actomyosin cytoskeleton by β-catenin, which binds to the cadherin cytoplasmic tail and to α-catenin, which in turn binds to F-actin[3–4] (Figure 1 (A)). This molecular linkage maintains tension at cell–cell contacts[5–6], and is essential for dynamic mechanical coupling between cells during morphogenesis and for tissue homeostasis.[1,5,7–10] During these and other processes, cell-generated forces

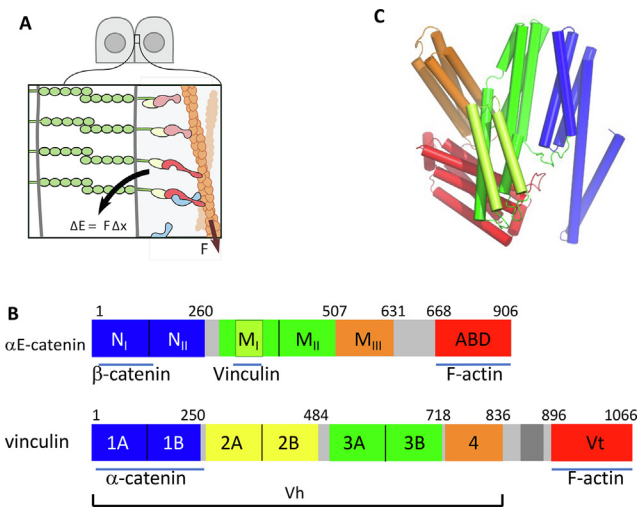

Figure 1. αE-catenin and vinculin at cell–cell contacts. (A) Schematic of a minimal cell–cell contact containing a classical cadherin (green), β-catenin (yellow), αE-catenin (red) and actin. Vinculin (blue) is recruited to the contact upon application of tension to αE-catenin. **(B)** Primary structures of αE-catenin *(top)* and vinculin *(bottom).* The N-terminal domain of αE-catenin, which binds β-catenin, contains two four-helix bundles, N_I and N_{II}.[45,67–69] The M domain consists of three four-helix bundles, designated M_I, M_{II} and M_{III}. The C-terminal ABD is a five-helix bundle. The vinculin N-terminal D1 domain confers full binding affinity for αE-catenin.[28] The head region spans domains 1–4. **(C)** Crystal structure of αE-catenin 82–906.[68]

must be coordinated and transmitted across tissues. In particular, cables of contractile filamentous (F)-actin and nonmuscle myosin II spanning multiple cells drive large-scale tissue rearrangements during embryonic development and wound healing.[11–15] The sarcomeric actomyosin arrays that power muscle contraction in the heart are similarly linked by cadherin-catenin complexes at cardiomyocyte cell–cell junctions. How these intercellular connections self-assemble, and how they remain stable under mechanical load, is unclear.

The ternary epithelial (E)-cadherin/β-catenin/αE(epithelial)-catenin complex binds transiently to F-actin,[16–17] but binding is strengthened by mechanical force, a property known as a catch bond, which is thought to reinforce intercellular contacts under tension.[18–20] In addition to the minimal ternary cadherin/β-catenin/α(E)-catenin complex, other proteins bind to αE-catenin and F-actin depending on the mechanical environment of the junction.[21–23] The best-studied example is vinculin, a paralog of αE-catenin found in focal adhesions and cell–cell junctions (Figure 1(B)). Vinculin is recruited to cell–cell junctions upon application of force to αE-catenin[24–26], where it strengthens the adhesive contact between cells.[27] In solution, both the N-terminal D1 domain of vinculin and the larger vinculin "head" (designated Vh) comprising all but its actin-binding domain (Figure 1(B)), bind αE-catenin or its complex with E-cadherin and β-catenin with modest affinity (K_D = ~2 μM) whereas both fragments bind to the isolated M_I-M_{II} fragment of αE-catenin with high affinity (K_D = ~15 nM).[28] Mechanical tension on αE-catenin is thought to reversibly displace intramolecular interactions within the M domain,[29] exposing the αE-catenin M_I subdomain and allowing it to bind strongly to vinculin.[28,30] Here, we explore the consequences of vinculin binding on the interaction of the cadherin-catenin complex with F-actin.

Results

The ternary complex shows asymmetric force-dependent binding to actin

We employed an optical trap (OT) assay[18,31–32] to compare the behavior of the ternary E-cadherin/β-catenin/αE-catenin complex with the quaternary complex formed by adding the vinculin head (Figure 2(A)). In this assay, a biotinylated actin filament is attached to two streptavidin-coated beads, which are each captured in an optical trap. This actin "dumbbell" is positioned over a platform displaying immobilized recombinant cadherin/catenin/(vinculin) complexes (Figure 2(A)). The stage is then moved back-and-forth approximately parallel to the filament. If an αE-catenin molecule attaches to the filament, stage motion pulls a bead out of its trap. When a bead displacement is detected, designated here as an "event", the stage movement is halted, leaving the complex under tension due to the restoring force of the trap, which acts as a simple spring that pulls the bead back to the waist of the laser beam. Note that the assay does not directly detect the presence of binding interactions of "bystander" complexes that bear little or no load, as these would not affect the positions of the optically

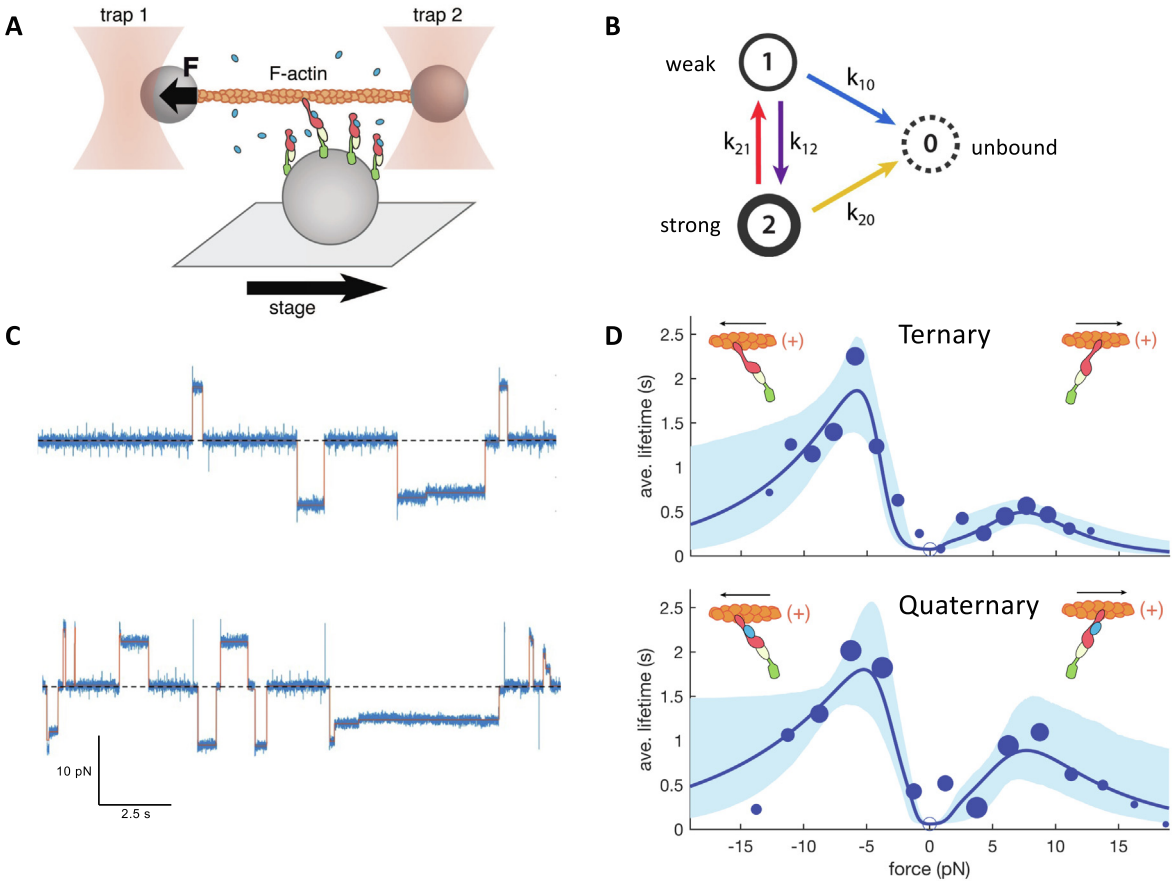

Figure 2. Force-dependent binding of cadherin/catenin complexes to F-actin. (A) Schematic of the OT assay. **(B)** The two-state catch bond model used in this work. Weak and strong actin-bound states 1 and 2 can interconvert, and either can dissociate from actin. Force promotes the transition between the weakly bound and strongly bound states, and also disfavors the transition from the strong to the weak state. **(C)** Representative OT data of the ternary (upper) and quaternary (lower) complexes. The zero-force baseline is shown as a dashed line. The assignment of filament direction is described in Supplemental Information. **(D)** Mean binding lifetimes (blue circles) and best-fit model (blue curve) for the ternary E-cadherin cytoplasmic domain/β-catenin/αE-catenin (upper plot) and quaternary E-cadherin cytoplasmic domain/β-catenin/αE-catenin/Vh (lower plot) derived from the last step data. Negative and positive values of force correspond to forces directed towards the (−) or (+) and of the filament, respectively. Areas of the circles are proportional to the number of events measured in each 2 pN bin. Open circle at force = 0 represents the constraint for the binding lifetime at low forces measured using a separate assay. The (+) symbol in the inset cartoon denotes the (+) end of the actin filament. Solid curves are the fit of the two-state catch bond model to the data, and the lighter envelope is the 95% confidence interval obtained by bootstrapping.

trapped beads. When a load-bearing complex detaches from the filament, the force from that attachment is lost, thereby providing measures of both the force and how long the attachment lasted. Most events had multiple steps in force before returning to baseline, which is interpreted in this study as successive releases of individual complexes (see Supplemental Discussion), such that the last step before all tension is lost corresponds to that of a single load-bearing complex. Steps observed for the quaternary complex are unlikely to arise from step transitions due to αE-catenin unfolding, as the αE-catenin M domain must adopt an open conformation to enable Vh binding. To examine the possibility of some steps arising from M-domain unfolding under force for the ternary complex, we compared step size distributions for the ternary and quaternary complexes and found them to be indistinguishable (Figure S4). Monte Carlo simulations (Figure S6) likewise indicate that steps due to M-domain unfolding are predicted to make minimal contributions to the observed step lifetime distributions due to their relative rarity.

The bound lifetimes of single load-bearing complexes had a biexponential distribution at any given force, indicating distinct short- and long-lived states.[18,31] This observation is consistent with a two-state catch bond[33–34] in which force increases

the rate of formation of a strong-binding state to actin and decreases the back reaction to the weak state (Figure 2(B)).[18,31] (In keeping with prior usage, we use 'weak' and 'strong' to denote distinct short- and long-lived binding states.[33–35]) The rates of interconversion between these states are described by the Bell-Evans model,[36–37] wherein the rate of a transition k_{ij} between states i and j = k_{ij}^{0} exp (Fx_{ij} / k_BT) where k_{ij}^{0} is the rate at zero force, F is the force magnitude, and x_{ij} is projection of the force vector onto the reaction coordinate r_{ij} (see below). Large values of x_{ij} indicate a high degree of force sensitivity and imply a large underlying structural transition.

Using an improved OT setup and determining the polarity of the filament by measuring the direction of its movement in a separate flow channel containing the pointed (−) end directed motor myosin VI,[31] we demonstrated that vinculin itself shows catch bond behavior that is asymmetric: its lifetime bound to F-actin is longer when force is directed towards the pointed (−) end of the actin filament than toward the barbed (+) end.[31] Asymmetric catch bond behavior was also recently reported for αE-catenin alone and for αE-catenin bound to β-catenin.[38] We therefore re-measured the force-dependent association of the ternary complex comprising the E-cadherin cytoplasmic domain, β-catenin, and αE-catenin with F-actin (Figure 2(C)). As before, analysis of the last step data revealed biphasic lifetimes at a given force (Figure S1). The lifetimes of the bound complex increase with force up to about 6–7 pN, and show asymmetry, with longer bound lifetimes when force is directed towards the (−) end (Figure 2(C, D); Supplemental Information). The asymmetric catch bond mechanism was recently rationalized based on the structure of the αE-catenin actin-binding domain (ABD) bound to F-actin[39] and validated in single molecule experiments.[32] We modeled these effects by directionally-dependent distance parameters, $x_{ij}^{(-)}$ and $x_{ij}^{(+)}$, denoting distance parameters for when force is oriented toward the F-actin (−) or (+) end, respectively (Supplemental Information, Table S1).

Effect of vinculin on cadherin/catenin complex binding to actin

To assess the effect of vinculin on the actin-binding activity of the ternary cadherin/catenin complex, we performed the OT assay on the quaternary E-cadherin/β-catenin/αE-catenin/vinculin complex made with the vinculin head (Vh), which lacks the vinculin actin-binding domain but contains the binding site for αE-catenin[28] (Figure 1(B), Figure S2). Vh was added at 15 μM to ensure that the cadherin/catenin complex will be nearly saturated with the vinculin head (see Methods), such that αE-catenin adopts an open conformation. Differences in last-step lifetimes for the ternary and quaternary complexes were modest, if at all present (Figure 2(C, D), Figure S3).

In cells, the cadherin-catenin complex assembles into large, hierarchically organized clusters,[40–42] but how multiple cadherin-catenin complexes might interact when binding to the same actin filament under load has not been examined. Therefore, binding lifetimes were quantified when multiple cadherin-catenin complexes simultaneously interacted with F-actin (Figure 3). When force was directed towards the (+) end of F-actin, the mean binding lifetime for each additional bound ternary or quaternary complex stayed constant (Figure 3(B)). When force was directed towards the (−) end of F-actin, the lifetimes for each additional ternary complex stayed constant or decreased. (Figure 3(C), Table S2). In contrast, the mean binding lifetime for each additional quaternary complex increased as a function of the number of load-bearing complexes interacting with the filament (Figure 3(C), Table S2). The mean forces for each step were similar for both the ternary and quaternary complex (Table S2) and could not explain this observation.

Behavior of multiple actin-bound complexes

Structural and biochemical studies[39,43] found direct contacts between actin-bound αE-catenin ABDs, and suggested that these interactions enhance binding between αE-catenin and F-actin. Cooperative binding of αE-catenin to F-actin was also reported in solution[44] and in a biophysical study wherein a single β-catenin/αE-catenin heterodimer formed a short-lived slip bond, but a higher heterodimer surface density enabled the complex to form a directional catch bond with F-actin.[38] Studies from our laboratories likewise indicate that interactions between neighboring cadherin-catenin complexes facilitates F-actin binding under load.[18,32] These observations suggest that entry into a long-lived binding state may be facilitated by interactions between neighboring complexes. However, to our knowledge how multiple cadherin-catenin complexes interact when under load had not been examined in detail.

To address this question, we first used Monte Carlo simulations based on kinetic parameters derived from the OT experiments to examine how load might be distributed when more than one complex is bound to F-actin. For simplicity, we considered two limiting, hypothetical cases: (1) load is shared equally among actin-bound complexes or (2) essentially all of the load is borne by a single complex, with the remainder bearing negligible load. Contrary to what is experimentally observed, in the equal load sharing model the average binding time per complex decreases (Figure S7(a)), because dividing the load among complexes tends to shift all of them into the weak-binding regime that predominates below 5 pN. In contrast, a model in which one complex bears all of the load predicts binding lifetimes that are independent of the number of interacting complexes, which qualitatively matches

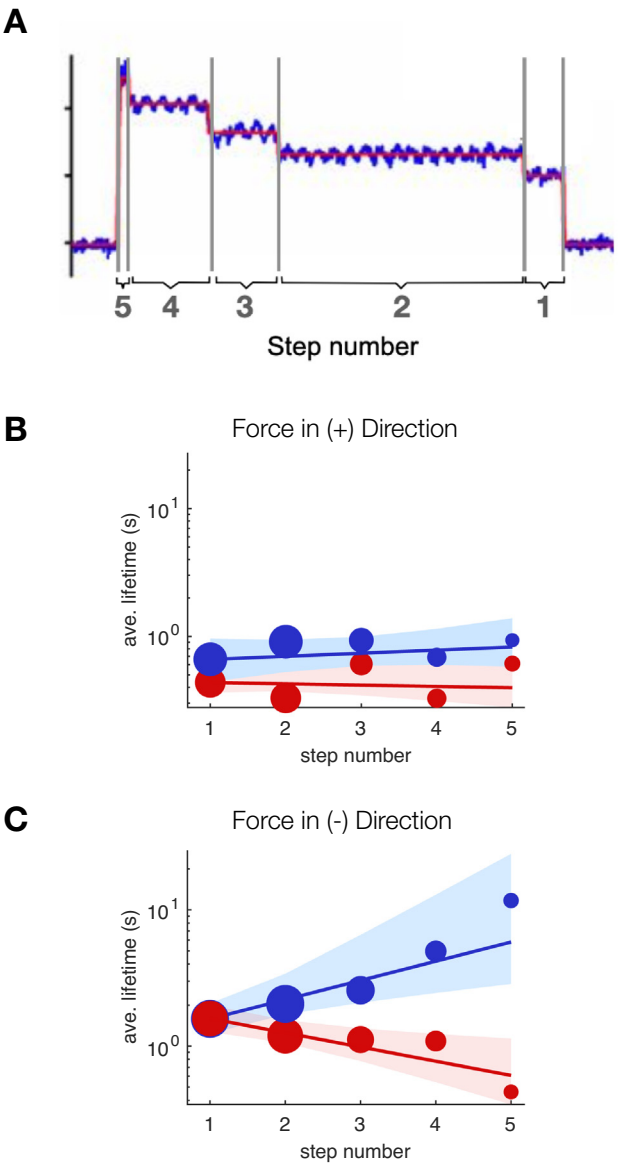

Figure 3. Binding of multiple complexes alters lifetime of individual bonds. (A) Duration of the Nth step, counting from the end of the trace. The 1st step corresponds to the last stairstep of the binding trace, such that only one load-bearing complex is bound. **(B, C)** The mean bound lifetimes for the quaternary complex (blue) and ternary complex (red) are shown as a function of the number of load-bearing complexes for an event, with load in the (+) and (-) directions, respectively. The size of the circles corresponds to the number of observations. The lines are fit to the function $L(n) = L_1 \exp(c \cdot (n-1))$, where $L(n)$ is the expected lifetime for a step number n, L_1 is the lifetime of the first-from-end step (*i.e.*, last step), and c a constant (see SI text). The envelopes represent the 95% confidence interval obtained by bootstrapping.

experimental observations for the ternary complex and for the quaternary complex when load was oriented towards the filament (+) end. In this model, all other bound complexes act as "bystanders" that are subject to negligible load, and that undergo cycles of detachment and rebinding. Note that in reality, "bystander" complexes must necessarily be subject to non-zero load due to their attachment to the filament, but may experience much smaller loads relative to the principal load-bearing complex, such that their dynamic, weak binding interactions with F-actin are unobservable in our assays. Nonetheless, the model in which load is placed on one complex at a time captures the main features of our data.

The fold increase in binding lifetime with step number is roughly constant (Figure 3(A)), which is consistent with a model in which load-bearing complex is progressively stabilized by an increasing number of neighboring complexes. As

a means of capturing this observation, we developed a hypothetical model in which neighbor-neighbor interactions lead to increased binding lifetimes (Figure 4). This model captures the data well (Figure S8). Remarkably, stabilization of only −1.5 k_BT per additional bound complex is sufficient to account for the observed increase in binding lifetimes (Figure S8), indicating that subtle effects can potentially lead to large increases in effective binding lifetimes (see Discussion).

Although neighbor-neighbor stabilization is physically plausible, it may not be the only contributor to the directional increase in bound-state lifetimes observed for the quaternary complex. For example, we examined an alternative scenario in which successive change in the angle of the applied force with the number of quaternary complexes interacting with F-actin might alter the degree to which applied load influences the balance between the weak and strong states (Supplemental Information, Figures S5 and S9). Successive changes in the angle of applied force as small as 5° also produce non-linear increase in binding lifetimes consistent with experimental observations. The inherent chirality of both F-actin and the quaternary complex makes it reasonable to suppose that this effect could occur in a direction-sensitive manner. Given their non-exclusivity, alterations in F-actin binding stability and these geometric effects may both contribute to the observed increase in binding lifetime, though we note that neither model has been experimentally verified.

To further explore the potential implications of cluster size and cooperative stabilization on actin binding, we calculated the *total time* elapsed until the last of the *N* complexes detached from the filament in Monte Carlo simulations, as a measure of force-dependent anchoring. For the ternary complex, total binding times at a given force scaled roughly linearly with *N* (Figure 5(A)). This is expected given that our data are best explained by a model in which a single complex bears the large majority of load at any given time (Figure 5 (E)). In contrast, cooperative stabilization in the quaternary complex leads to a large, nonlinear increase in binding lifetimes when load was oriented in the (−) direction (Figure 5(B)). Note that although the implementation in Figure 5 assumes neighbor-neighbor interactions as the basis for cooperative binding stabilization, any mechanism that yields a nonlinear increases in binding lifetimes with respect to cluster size would

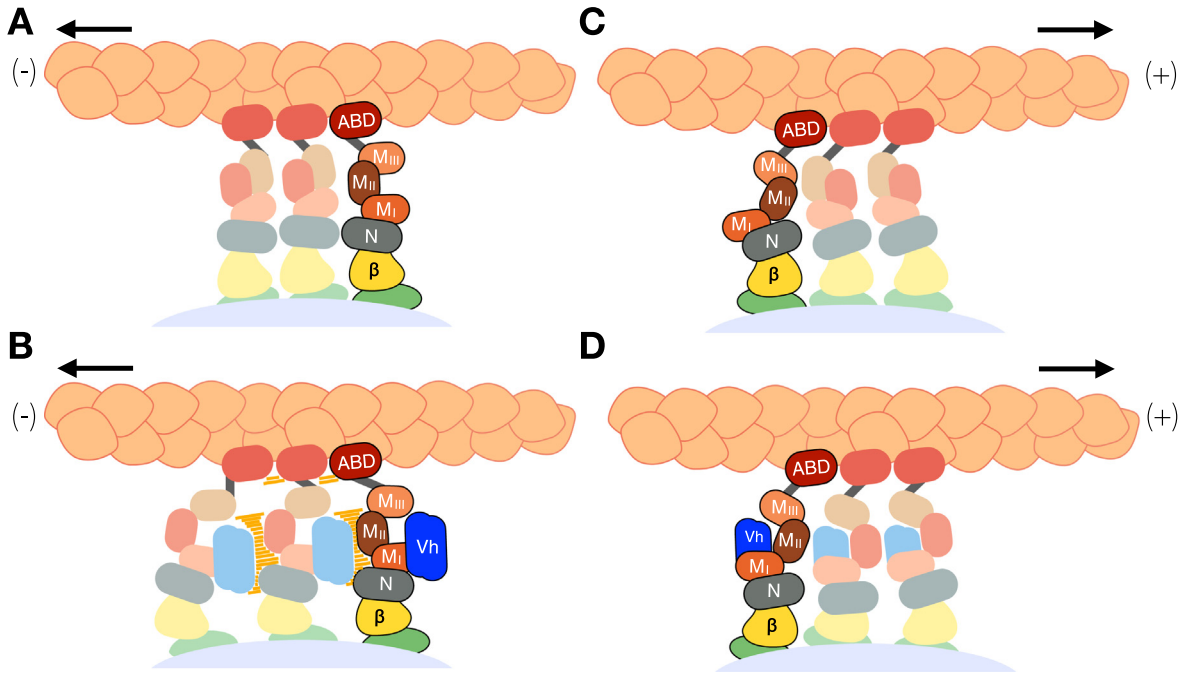

Figure 4. Possible mechanism of increased bound-state lifetimes of cadherin/catenin complexes with (−)-end directed force when vinculin is bound. E-cadherin cytoplasmic domain is shown in green, β-catenin in yellow, αE-catenin by its individual domains colored as in Figure 1, and Vh in blue. The lighter complexes represent bound complexes experiencing no or small load, whereas the darker complexes are experiencing significant load. (**A**, **B**) With force directed in the (−) direction, the M_{III} domain may adopt a position that allows it to contact a vinculin molecule bound to an adjacent complex (orange bars) or cause conformational changes in the ABD. (**C**, **D**) (+)-end directed force may produce a different position of M_{III} that cannot contact Vh bound to an adjacent complex or cause conformational changes that would alter binding lifetimes of the neighboring complex.

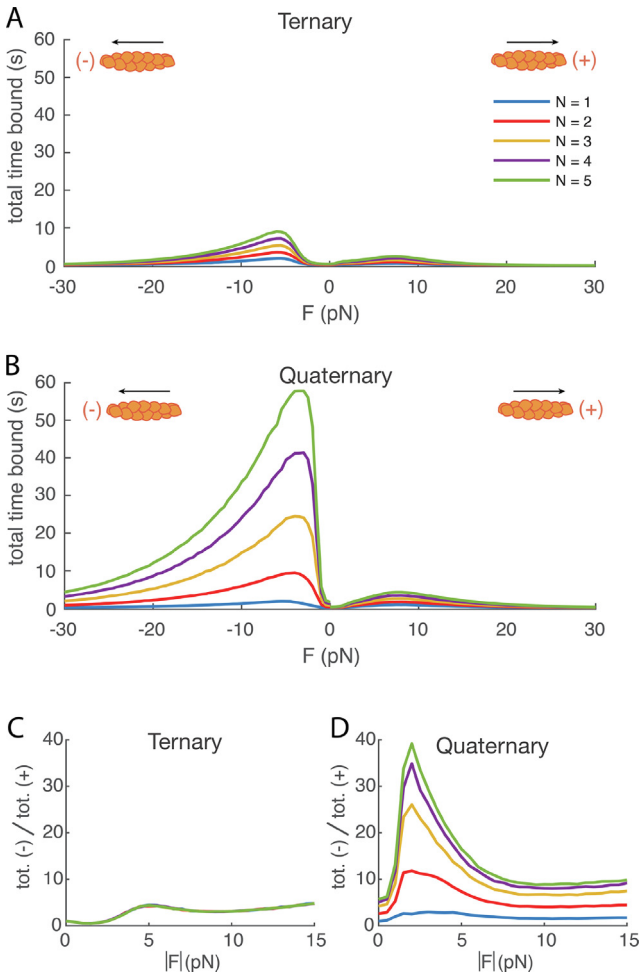

Figure 5. Effects of load sharing and cooperativity on force-dependent actin anchoring. (A) Monte Carlo simulation of the total duration until complete detachment for $N = 1$–5 ternary complexes, with force $\boldsymbol{F}$ oriented toward the F-actin (−) end. Detachment is modeled as irreversible. **(B)** Simulation as in (A) but for the quaternary complex. **(C)** Simulated ratio of the time until complete detachment for the ternary complex loaded in the (−) vs (+) directions. **(D)** Simulation as in (C) but for the quaternary complex. Cooperative interactions between complexes lead to a large, force-dependent increase in directionality. Note that, for the quaternary complex, lifetime ratios are not equal to 1 at zero force due to neighbor-neighbor stabilization when loaded in the (−) but not (+) direction. This represents an approximation of the more physically realistic case in which neighbor-neighbor stabilization may depend on both load direction and magnitude.

generate a similar result. This nonlinearity in turn leads to an asymmetry in binding lifetimes that increases rapidly with N for the quaternary, but not for the ternary complex (Figure 5(C, D)).

Discussion

We have shown that independent of its own actin-binding activity, vinculin profoundly alters force-dependent binding of multiple cadherin-catenin complexes to F-actin: association of vinculin with the ternary complex of E-cadherin, β-catenin and αE-catenin increases the bound lifetime of individual complexes on F-actin as a function of the number of load-bearing complexes bound, but only when force is directed towards the pointed (−) end of the filament. Thus, force not only promotes both strong binding of the ternary complex to F-actin and to vinculin, but also enables the now-bound vinculin to potentiate the polarization of F-actin. In this way, vinculin may enhance the stability of the cadherin/catenin/F-actin assembly with load, and thereby reinforce cell–cell contacts. In contrast, the ternary complex does not show this behavior. While it may be possible that some shorter steps observed in the ternary complex arise from M-domain unfolding rather than rupture events, the observed step size distributions are essentially identical to the quaternary complex, where force is not anticipated to induce protein unfolding (Figure S4).

Furthermore, we anticipate that the contributions from M domain unfolding to the observed step lifetime distribution should be minimal for the ternary complex (Figure S6).

The molecular mechanism(s) by which vinculin enhances cooperative and directional F-actin anchoring are unclear. The intrinsic chirality of F-actin and the αE-catenin ABD possibly enables cooperative stabilization to occur only when force is applied in the (−) direction. It is possible that this arises from favorable interactions between neighboring complexes, reorientation of load in a way that enhances the lifetime of the catch bond, or both (Figure 4, Figures S5 and S9). Vinculin binding requires unfolding of the αE-catenin M_I domain and the loss of interactions that stabilize the relative positions of M_I, M_{II}, and M_{III}.[28–29,45–47] This repositioning of domains may produce new, directionally dependent contacts between neighboring complexes that selectively stabilize actin-bound states depending on the orientation of the applied load (Figure 4(B, D)). Such neighbor-neighbor stabilization would likely not occur for ternary complexes, since all but the load-bearing complex would adopt the compact, noninteracting M domain conformation (Figure 4(A, C)). Given evidence for allosteric communication between the αE-catenin M-domain and ABD[32,46], it is possible that the directional repositioning of αE-catenin M subdomains when Vh is bound could allosterically alter ABD conformation and actin binding stability. It is likewise possible that the directionally dependent repositioning of αE-catenin domains alters the projection of force along the reaction coordinates that correspond to transitions between states of the ABD catch bond,[32] resulting in an increase in binding lifetimes as additional complexes are bound. Experimental tests of these models are, however, beyond the scope of this study.

Implications of unequal load sharing

When multiple cadherin/catenin complexes bind to an actin filament, it would be reasonable to expect that load would be shared equally among interacting complexes. Instead, we found that bound-state lifetimes for the ternary complex, as well as the quaternary complex when force is oriented in the (+) direction, are most easily explained by a model in which only one complex bears essentially all the load, with the rest acting as bystanders. For the quaternary complex, the increase in mean lifetimes as a function of number of load-bearing complexes when force is oriented in the (−) direction is also consistent with unequal load sharing, but with an additional source of stabilization that scales with the number of bound complexes. A possible explanation for unequal load sharing is that the force-extension behavior of the cadherin-catenin complex is nonlinear, *i.e.,* more analogous to a rope than a spring. In this view, whichever complex reaches its maximal extension first would bear the majority of the mechanical load. In integrin-based adhesions, a minority of integrins bear the majority of the load,[48] suggesting that unequal load-sharing may occur *in vivo*.

Depending on the total load and the force sensitivity of the catch bonds, unequal load sharing could provide a counterintuitive stabilization of the linkage between adhesion complexes and F-actin: one complex bearing most of the load yields nearly constant individual binding lifetimes regardless of the number of load-bearing complexes bound to F-actin, meaning that how long a filament stays attached to the adhesion complex scales linearly with the number of load-bearing complexes. If the total force per F-actin filament is similar to the catch bond maximum (∼6 pN for the cadherin-catenin complex), this can produce *longer* total binding lifetimes than equal load sharing, since in the latter case individual binding lifetimes decrease when load is spread among too many complexes (Figure S7). Consistent with this possibility, both the maximal force generated by nonmuscle myosin II (3.5 pN),[49] and the inferred forces transmitted by individual cytoskeletal linkers in living cells (∼4–8 pN)[48] are comparable to the force at which maximal binding lifetimes occur for the cadherin-catenin[18] and vinculin[31] catch bonds.

Possible consequences of asymmetric binding to F-actin

Contractile F-actin cables spanning multiple cells power embryonic morphogenesis and wound-healing in epithelia, and muscle contraction in the heart. The actin cables in some epithelial tissues show clear sarcomeric organization, implying that the barbed (+) ends of the filaments terminate at tricellular junctions[13,15,50–52] (Figure 6(C)). This arrangement is consistent with cell biological, genetic, and electron microscopy data indicating that actin filaments are anchored end-on at epithelial tricellular junctions (e.g. Refs. 53–54) Myosin II motor activity is required for the organization of these bundles as well as recruitment of cell–cell junction components.[15,55–59] An identical molecular-scale organization links myofibrils across the junctions between cardiomyocytes in the heart.[60] However, how these cables can self-assemble to span multiple cells has been unclear.

We propose that a positive feedback loop stabilizes the connection of the cable at cell–cell junctions (Figure 6(A, B)): (*i*) Load oriented toward the F-actin (−) end, as generated by nonmuscle myosin II, engages the cadherin-catenin complex catch bond, producing a modest bias in the orientation of the actin filaments. (*ii*) Tension on the cadherin-catenin complex leads to the recruitment of vinculin, yielding additional polarization due to the enhancement of binding lifetimes and directionality for multiple, vinculin-

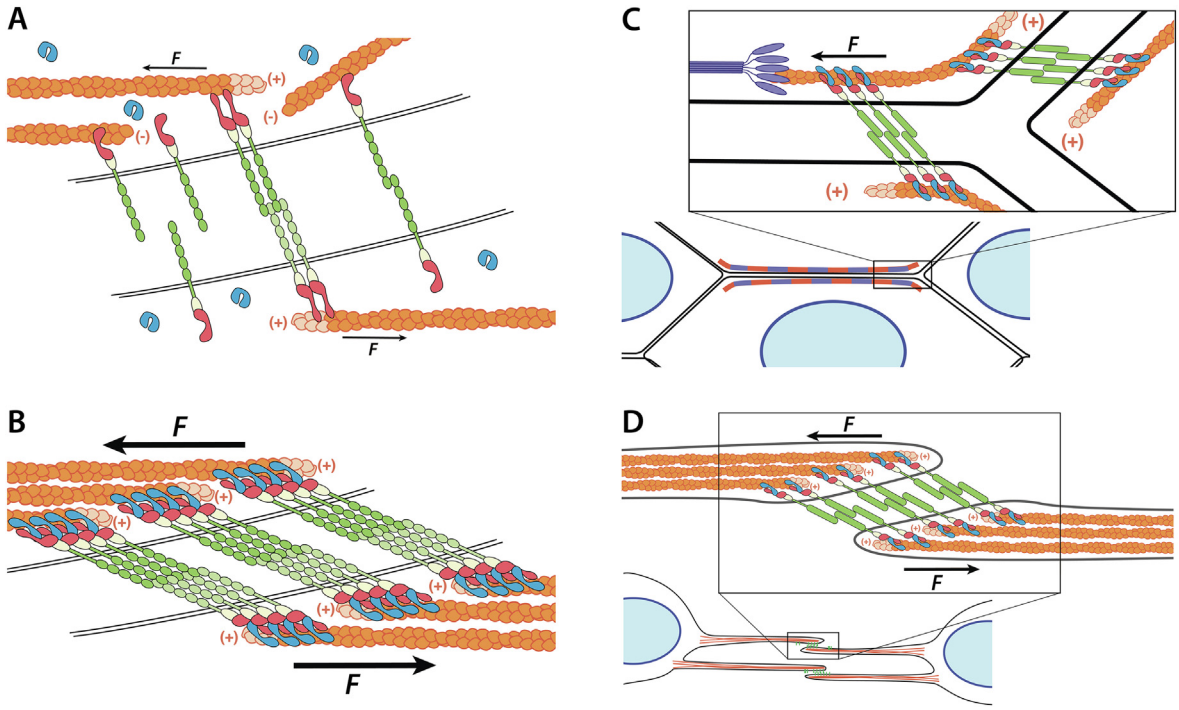

Figure 6. Possible model for assembly of load-bearing connections at cell–cell junctions. (A) At low forces, connections between F-actin (*orange*, new (+) ends *light orange*) and the α-catenin/β-catenin/E-cadherin complex (*red*, *yellow*, and *green*) are transient. Vinculin (*blue*) is predominantly in its autoinhibited and cytosolic. (**B**) Force above a threshold opens the vinculin binding site on α-catenin, recruiting vinculin. Cooperative interactions between neighboring quaternary complexes stabilize F-actin loaded toward the (−) end, and simultaneously favor cadherin clustering. **(C)** At tricellular junctions, load-stabilized cadherin-catenin clusters, as in (B), link contractile actin and myosin (*purple*) bundles spanning epithelial tissues. **(D)** Load-driven self-assembly stabilizes and organizes F-actin in contacting protrusions during the assembly of endothelial cell–cell junctions.

bound cadherin-catenin complexes. (*iii*) The force-dependent, directional bonds between vinculin and F-actin[31] impart additional polarization to local filaments. At each step, polarization of F-actin is anticipated to increase the efficiency of force generation by nonmuscle myosin II, leading to a positive feedback loop between myosin contractility, catch bond formation, and F-actin polarization. This feedback loop would result in the ordered sarcomeric assemblies observed in epithelia[13,15,61] and cardiomyocytes[60] (Figure 6(C)). However, the same feedback loop would be expected to stabilize actomyosin bundles of mixed polarity, though with effectiveness that is correspondingly reduced, given that myosin II can only exert force on filaments oriented with their (+) ends pointing away from the myosin bundle (Figure 6(C)). Importantly, myosin II organization appears to precede assembly of mature cell–cell junctions, consistent with the need for tension to promote the polarized binding of αE-catenin and vinculin to F-actin.[15,62]

Directional catch bonds may also play a wider role in driving cell and tissue organization. For example, the organization of F-actin predicted by our model (highly oriented, with barbed ends out) is observed at VE-cadherin based adhesions between the protrusions of neighboring endothelial cells[62–63] (Figure 6(D)). A recent study likewise demonstrates that talin, the principal F-actin binding protein in integrin-based adhesions, also forms a highly directional catch bond with F-actin,[64] suggesting a parallel mechanism for the formation of stress fibers to the one explored here. We speculate that directionally polarized binding interactions of the sort described in this study may constitute an important, and presently underexplored, organizing mechanism for the cytoskeleton.

Methods

Protein expression and purification

Mouse E-cadherin cytoplasmic domain, E-cadherin cytoplasmic domain aa 785–788, β-catenin, β-catenin 78–671, αE-catenin, and full length chicken vinculin were purified as described.[28,46] Vinculin head (Vh; residues 1–851) was expressed with a His_6 tag in a pET15b vector (kind gift from Dr. Susan Craig) and was purified as previously described.[65] Zebrafish αE-catenin

used in the OT experiments was purified as previously described.[66]

The expression vector for GFP-E-cadherin used in the OT assay was constructed by inserting DNA encoding the cytoplasmic domain of *Mus musculus* E-cadherin into the pPROEX HTb vector along with DNA encoding eGFP to generate an in-frame fusion consisting of an N-terminal His_6-tag, eGFP, and E-cadherin. GFP-E-cadherin was expressed in BL21(DE3) Codon Plus *E. Coli* cells in LB media at 37 °C. Cells were grown to an OD of 1.0 and induced with 0.5 mM IPTG. After induction, the cells were grown for 16 h at 18 °C, pelleted and resuspended in 20 mM Tris pH 8.0, 150 mM NaCl, 1 mM β-mercaptoethanol and flash frozen. Thawed cell pellets were lysed with an Emulsiflex cell disrupter in the presence of EDTA-free protease inhibitor cocktail set V (EMD Millipore) and Dnase (Sigma Aldrich). The lysate was centrifuged at 27,000*g* for 30 minutes. Clarified lysate from 2 L of cells was incubated with 10 mL of TALON Superflow resin (GE Healthcare Life Sciences) for 30 minutes on a rotator at 4 °C. Protein was washed with 5 bed volumes of 20 mM Tris pH 8.0, followed by 5 bed volumes of bed volumes of PBS pH 8.0, 0.5 M NaCl, 0.005% Tween 20, followed by 3 volumes of 20 mM Tris pH 8.0, 150 mM NaCl, 10 mM imidazole, 1 mM β-mercaptoethanol. Protein was eluted from the TALON resin in 20 mM Tris pH 8.0, 150 mM imidazole, 100 mM NaCl, 1 mM β-mercaptoethanol. The eluate was passed through a 0.22 μm SFCA syringe filter and diluted to a final volume of 50 mL in 20 mM Tris pH 8.0, 1 mM DTT, 0.5, mM EDTA. The filtered eluate was applied to a MonoQ anion exchange column in 20 mM Tris, pH 8.0, 1 mM DTT and run with a 0–1 M NaCl gradient and protein eluted at approximately 300 mM NaCl.

Proteins were stored at −80 °C and never underwent more than one freeze/thaw cycle.

Optical trap assay

In this assay a biotinylated actin filament links two optically-trapped, streptavidin-coated beads to create a "dumbbell" (Figure 2(A)). The actin filament is then positioned over a surface-immobilized "platform" bead bearing cadherin/β-catenin/αE-catenin complexes. The microscope stage is moved in a trapezoid-wave pattern, such that the binding of complexes on the platform bead results in the displacement of one of the two optically trapped beads (Figure 2(A)). The stage motion stops if a binding event is detected at the end of a 5 ms loading phase.

When a displacement is detected, the stage motion halts and the displaced bead relaxes back to its equilibrium position as the bound complexes release from the filament. The last release step corresponds to the dissociation time of a single complex. Because the optical trap acts as a spring with a known stiffness, the displacement provides the force exerted on the bead. Once both optically trapped beads return to their baseline position, the stage motion resumes, allowing us to record multiple such binding events per platform bead.

The optical trap assay was carried out as described,[18] with 50 μM GFP-E-cadherin cytoplasmic domain, 100 nM β-catenin, and 75 nM αE-catenin, except the final buffer injection also included 1 μM Trolox (Sigma Aldrich). Zebrafish αE-catenin was used in these experiments to ensure that only monomeric αE-catenin was added.[18] For vinculin experiments, 15 μM of Vh was added in the final injection. This concentration was chosen based on the K_D of 1.9 μM of the vinculin D1 domain for the ternary complex in solution,[28] which implies that approximately 90% of the complexes would be bound to vinculin in the absence of force. Vinculin-binding locks the αE-catenin in an open conformation, with a dissociation rate of $< 10^{-5}$ s^{-1}.[29] We were unable to obtain a direct ITC measurement of the affinity of Vh for the ternary complex, likely because the enthalpy change is very small, as found for D1,[28] but since both Vh and D1 bind to the minimal vinculin-binding fragment of αE-catenin with similar affinities,[28] we assume that their affinities for the wild-type complex are comparable. Importantly, force promotes binding of vinculin to αE-catenin,[29] so the effective K_D in the OT experiments is likely to be higher. Control experiments in which Vh or buffer alone was added to the flow cell containing beads bearing cadherin cytoplasmic domain and β-catenin, but no αE-catenin, showed no significant binding to F-actin.

Every binding interaction which survived the 5 ms load phase was included. We used the previously described directionality assay[31] to determine the polarity of a subset of the actin filaments, and used this subset to infer the directionality of all of the filaments that had sufficient data to be statistically significant (see SI text). Modeling of the data was constrained such that the mean lifetime at zero force was less than or equal to the mean lifetime measured using a low-force OT binding assay, as previously described.[31]

Selection of two-state catch bond model and statistical analysis

To model the OT data, one-state slip and catch bond models, as well as a two-state slip bond model, described previously,[18,31] were considered. One-state models were ruled out because they could not capture the biexponential distribution of lifetimes at a given force. The two-state slip bond model was ruled out because it cannot describe the biphasic behavior of the force-lifetime curve. Details of the two-state directional catch bond model, statistical analysis and parameters are provided in Supplementary information and Table S1.

Simulations

Details of the Monte Carlo simulations are provided in the SI.

DATA AVAILABILITY

Data will be made available on request.

Received 10 May 2022;
Accepted 11 January 2023;
Available online 20 January 2023

Keywords:
cytoskeleton;
single molecule force spectroscopy;
cell-cell adhesion;
mechanotransduction;
kinetic modeling

Acknowledgements

We thank Dr. Craig Buckley for his contributions to the early stages of this project. Research reported in this publication was supported by a Howard Hughes Medical Institute Faculty Scholar Award (A.R.D), as well as National Institutes of Health grant R01GM114462 to W.I.W. and A.R.D, R35GM130332 to A.R.D. and R35GM131747 to W.I.W. N.A.B. and D.L.H. were supported by training grant T32 GM007276 from the NIH. A.W. and D.L.H. were supported by Graduate Fellowships from the National Science Foundation. A.W. was also supported by a Stanford Graduate Fellowship and training grant T32GM120007. Use of the Stanford Synchrotron Radiation Lightsource, SLAC National Accelerator Laboratory, is supported by the U.S. Department of Energy, Office of Science, Office of Basic Energy Sciences under Contract No. DE-AC02-76SF00515. The SSRL Structural Molecular Biology Program is supported by the Department of Energy Office of Biological and Environmental Research and by the National Institutes of Health, NIGMS Grant P30GM133894. The contents of this publication are solely the responsibility of the authors and do not necessarily represent the official views of NIGMS or NIH.

Data availability

The OT data, analysis scripts and modeling computer code used in this work are available upon reasonable request from the corresponding authors.

Declaration of interests

The authors declare that they have no known competing financial interests or personal relationships that could have appeared to influence the work reported in this paper.

Appendix A. Supplementary material

Supplementary material to this article can be found online at https://doi.org/10.1016/j.jmb.2023.167969.

† These authors contributed equally to this study.

References

1. Pinheiro, D., Bellaiche, Y., (2018). Mechanical force-driven adherens junction remodeling and epithelial dynamics. *Dev. Cell* **47**, 3–19.
2. Nishimura, T., Takeichi, M., (2009). Remodeling of the adherens junction during morphogenesis. *Curr. Top. Dev. Biol.* **89**, 33–54.
3. Shapiro, L., Weis, W.I., (2009). Structure and biochemistry of cadherins and catenins. *Cold Spring Harb. Perspect. Biol.* **1**, a003053
4. Pokutta, S., Weis, W.I., (2007). Structure and mechanism of cadherins and catenins in cell-cell contacts. *Annu. Rev. Cell Dev. Biol.* **23**, 237–261.
5. Cavey, M., Lecuit, T., (2009). Molecular bases of cell-cell junctions stability and dynamics. *Cold Spring Harb. Perspect. Biol.* **1**, a002998
6. Borghi, N., Sorokina, M., Shcherbakova, O.G., Weis, W.I., Pruitt, B.L., Nelson, W.J., et al., (2012). E-cadherin is under constitutive actomyosin-generated tension that is increased at cell-cell contacts upon externally applied stretch. *PNAS* **109**, 12568–12573.
7. Perez-Moreno, M., Jamora, C., Fuchs, E., (2003). Sticky business: orchestrating cellular signals at adherens junctions. *Cell* **112**, 535–548.
8. Stepniak, E., Radice, G.L., Vasioukhin, V., (2009). Adhesive and signaling functions of cadherins and catenins in vertebrate development. *Cold Spring Harb. Perspect. Biol.* **1**, a002949
9. Martin, A.C., Gelbart, M., Fernandez-Gonzalez, R., Kaschube, M., Wieschaus, E., (2010). Integration of contractile forces during tissue invagination. *J. Cell Biol.* **188**, 735–749.
10. Dufour, S., Mege, R.M., Thiery, J.P., (2013). α-catenin, vinculin, and F-actin in strengthening E-cadherin cell-cell adhesions and mechanosensing. *Cell Adh. Migr.* **7**, 345–350.
11. Miao, H., Blankenship, J.T., (2020). The pulse of morphogenesis: actomyosin dynamics and regulation in epithelia. *Development* **147**, dev186502.
12. Yonemura, S., Itoh, M., Nagafuchi, A., Tsukita, S., (1995). Cell-to-cell adherens junction formation and actin filament organization: similarities and differences between non-polarized fibroblasts and polarized epithelial cells. *J. Cell Sci.* **108**, 127–142.
13. Ebrahim, S., Fujita, T., Millis, B.A., Kozin, E., Ma, X., Kawamoto, S., et al., (2013). NMII Forms a contactile

transcellular sarcomeric network to regulate apical cell junctions and tisue geometry. *Curr. Biol.* **23**, 731–736.
14. Li, J.X.H., Tang, V.W., Boateng, K.A., Brieher, W.M., (2021). Cadherin puncta are interdigitated dynamic actin protrusions necessary for stable cadherin adhesion. *Proc. Natl. Acad. Sci. U.S.A.* **118**, e2023510118
15. Yu-Kemp, H.C., Szymanski, R.A., Cortes, D.B., Gadda, N. C., Lillich, M.L., Maddox, A.S., et al., (2022). Micron-scale supramolecular myosin arrays help mediate cytoskeletal assembly at mature adherens junction. *J. Cell Biol.* **221**, e202103074.
16. Drees, F., Pokutta, S., Yamada, S., Nelson, W.J., Weis, W. I., (2005). α-Catenin is a molecular switch that binds E-cadherin/β-catenin and regulates actin filament assembly. *Cell* **123**, 903–915.
17. Yamada, S., Nelson, W.J., (2007). Localized zones of Rho and Rac activities drive initiation and expansion of epithelial cell-cell adhesion. *J. Cell Biol.* **178**, 517–527.
18. Buckley, C.D., Tan, J., Anderson, K.L., Hanein, D., Volkmann, N., Weis, W.I., et al., (2014). The minimal cadherin-catenin complex binds to actin filaments under force. *Science* **346**, 1254211.
19. Dembo, M., Torney, D.C., Saxman, K., Hammer, D., (1988). The reaction-limited kinetics of membrane-to-surface adhesion and detachment. *Proc. R. Soc. Lond. B Sci.* **234**, 55–83.
20. Marshall, B.T., Long, M., Piper, J.W., Yago, T., McEver, R. P., Zhu, C., (2003). Direct observation of catch bonds involving cell-adhesion molecules. *Nature* **423**, 190–193.
21. Taguchi, K., Ishiuchi, T., Takeichi, M., (2011). Mechanosensitive EPLIN-dependent remodeling of adherens junctions regulates epithelial reshaping. *J. Cell Biol.* **194**, 643–656.
22. Yu, H.H., Zallen, J.A., (2020). Abl and Canoe/Afadin mediate mechanotransduction at tricellular junctions. *Science* **370**, eaba5528.
23. Sakakibara, S., Mizutani, K., Sugiura, A., Sakane, A., Sasaki, T., Yonemura, S., et al., (2020). Afadin regulates actomyosin organization through αE-catenin at adherens junctions. *J. Cell Biol.* **219**, e201907079.
24. le Duc, Q., Shi, Q., Blonk, I., Sonnenberg, A., Wang, N., Leckband, D., et al., (2010). Vinculin potentiates E-cadherin mechanosensing and is recruited to actin-anchored sites within adherens junctions in a myosin II-dependent manner. *J. Cell Biol.* **189**, 1107–1115.
25. Yonemura, S., Wada, Y., Watanabe, T., Nagafuchi, A., Shibata, M., (2010). α-Catenin as a tension transducer that induces adherens junction development. *Nature Cell Biol.* **12**, 533–542.
26. Kim, T.J., Zheng, S., Sun, J., Muhamed, I., Wu, J., Lei, L., et al., (2015). Dynamic visualization of α-catenin reveals rapid, revesible conformation switching between tension states. *Curr. Biol.* **25**, 218–224.
27. Thomas, W.A., Boscher, C., Chu, Y.S., Cuvelier, D., Martinez-Rico, C., Seddiki, R., et al., (2013). α-Catenin and vinculin cooperate to promote high E-cadherin-based adhesion strength. *J. Biol. Chem.* **288**, 4957–4969.
28. Choi, H.J., Pokutta, S., Cadwell, G.W., Bobkov, A.A., Bankston, L.A., Liddington, R.C., et al., (2012). αE-catenin is an autoinhibited molecule that coactivates vinculin. *PNAS* **109**, 8576–8581.
29. Yao, M., Qiu, W., Liu, R., Efremov, A.K., Cong, P., Seddiki, R., et al., (2014). Force-dependent conformational switch of α-catenin controls vinculin binding. *Nature Commun.* **5**, 4525.
30. Rangarajan, E.S., Izard, T., (2012). The cytoskeletal protein α-catenin unfurls upon binding to vinculin. *J. Biol. Chem.* **287**, 18492–18499.
31. Huang, D.L., Bax, N.A., Buckley, C.D., Weis, W.I., Dunn, A. R., (2017). Vinculin forms a directionally asymmetric catch bond with F-actin. *Science* **357**, 703–706.
32. Wang, A., Dunn, A.R., Weis, W.I., (2022). Mechanism of the cadherin-catenin F-actin catch bond interaction. *eLife* **11**, e80130.
33. Barsegov, V., Thirumali, D., (2005). Dynamics of unbinding of cell adhesion molecules: transition from catch to slip bonds. *PNAS* **102**, 1835–1839.
34. Thomas, W.E., Forero, M., Yakovenko, O., Nilsson, L., Vicini, P., Sokurenko, E., et al., (2006). Catch-bond model derived from allostery explains force-activated bacterial adhesion. *Biophys. J.* **90**, 753–764.
35. Imamura, Y., Itoh, M., Maeno, Y., Tsukita, S., Nagafuchi, A., (1999). Functional domains of α-catenin required for the strong state of cadherin-based cell adhesion. *J. Cell Biol.* **144**, 1311–1322.
36. Bell, G.I., (1978). Models for the specific adhesion of cells to cells. *Science* **200**, 618–627.
37. Evans, E., (2001). Probing the relation between force-lifetime-and chemistry in single molecular bonds. *Annu. Rev. Biophys. Biomol. Struct.* **30**, 105–128.
38. Arbore, C., Sergides, M., Gardini, L., Bianchi, G., Kashchuk, A.V., Pertici, I., et al., (2022). α-catenin switches between a slip and an asymmetric catch bond with F-actin to cooperatively regulate cell junction fluidity. *Nature Commun.* **13**, 1146.
39. Xu, X.P., Pokutta, S., Torres, M., Swift, M.F., Hanein, D., Volkmann, N., et al., (2020). Structural basis of αE-catenin–F-actin catch bond behavior. *Elife* **9**, e60878.
40. Bertocchi, C., Wang, Y., Ravasio, A., Hara, Y., Wu, Y., Sailov, T., et al., (2017). Nanoscale architecture of cadherin-based cell adhesions. *Nature Cell Biol.* **19**, 28–37.
41. Quang, B.T., Mani, M.A., Markova, O., Lecuit, T., Lenne, P. F., (2013). Principles of E-cadherin supramolecular organization in vivo. *Curr. Biol.* **23**, 2197–2207.
42. Wu, Y., Kanchanawong, P., Zaidel-Bar, R., (2015). Actin-delimited adhesion-independent clustering of E-cadherin forms the nonoscale building blocks of adherens junctions. *Dev. Cell* **32**, 139–154.
43. Mei, L., Espinosa de los Reyes S, Reynolds MJ, Liu S, Alushin GM., (2020). Molecular mechanism for direct actin force-sensing by α-catenin. *Elife* **9**, e62514.
44. Hansen, S.D., Kwiatkowski, A.V., Ouyang, C.Y., Liu, H., Pokutta, S., Watkins, S.C., et al., (2013). αE-catenin actin-binding domain alters actin filament conformation and regulates binding of nucleation and disassembly factors. *Mol. Biol. Cell* **24**, 3710–3720.
45. Ishiyama, N., Tanaka, N., Abe, K., Yang, Y.J., Abbas, Y.M., Umitsu, M., et al., (2013). An autoinhibited structure of α-catenin and its implications for vinculin recruitment to adherens junctions. *J. Biol. Chem.* **288**, 15913–15925.
46. Terekhova, K., Pokutta, S., Kee, Y.S., Li, J., Tajkhorshid, E., Fuller, G., et al., (2019). Binding partner- and force-

promoted changes in αE-catenin conformation probed by native cysteine labeleing. *Sci. Rep.* **9**, 15375.
47. Hirano, Y., Amano, Y., Yonemura, S., Hakoshima, T., (2018). The force-sensing device region of α-catenin is an intrinsically disordered segment in the absence of intramolecular stabilization of the autoinhibitory form. *Genes Cells* **23**, 370–385.
48. Tan, S.J., Chang, A.C., Anderson, S.M., Miller, C.M., Prahl, L.S., Odde, D.J., et al., (2020). Regulation and dynamics of force transmission at individual cell-matrix adhesion bonds. *Sci. Adv.* **6**, eaax0317.
49. Hundt, N., Steffen, W., Pathan-Chhatbar, S., Taft, M.H., Manstein, D.J., (2016). Load-dependent modulation of non-muscle myosin-2A function by tropomyosin 4.2. *Sci. Rep.* **6**, 20554.
50. Coravos, J.S., Martin, A.C., (2016). Apical sarcomere-like actomyosin contracts nonmuscile Drosophila epithelial cells. *Dev. Cell* **39**, 346–358.
51. Houssin, N.S., Martin, J.B., Coppola, V., Yoon, S.O., Plagaeman, T.F.J., (2020). Formation and contraction of multicellular actomyosin cables facilitate lens placode invagination. *Dev. Biol.* **462**, 36–49.
52. Gomez, G.A., McLachlan, R.W., Wu, S.K., Caldwell, B.J., Moussa, E., Verma, S., et al., (2015). An RPTPa/Src family kinase/Rap1 signaling moedule recruits myosin IIB to support contractile tension at apical E-cadherin junctions. *Mol. Biol. Cell* **26**, 1249–1262.
53. Choi, W., Acharya, B.R., Peyret, G., Fardin, M.A., Mege, R. M., Ladoux, B., et al., (2016). Remodeling the zonula adherens in response to tension and the role of afadin in this response. *J. Cell Biol.* **213**, 243–260.
54. Yonemura, S., (2011). Cadherin-actin interactions at adherens junctions. *Curr. Opin. Cell Biol.* **23**, 515–522.
55. Verkhovsky, A.B., Svitkina, T.M., Borisy, G.G., (1995). Myosin II filament assemblies in the active lamella of fibroblasts: their morphogenesis and role in the formation of actin filament bundles. *J. Cell Biol.* **131**, 989–1002.
56. Miyake, Y., Inoue, N., Nishimura, K., Kinoshita, N., Hosoya, H., Yonemura, S., (2006). Actomyosin tension is required for correct recruitment of adherens junction components and zonula occludens formation. *Exp. Cell Res.* **312**, 1637–1650.
57. Smutny, M., Cox, H.L., Leerberg, J.M., Kovacs, E.M., Conti, M.A., Ferguson, C., et al., (2010). Myosin II isoforms identify distinct functional modules that support integrity of the epithelial zonula adherens. *Nature Cell Biol.* **12**, 696–702.
58. Leerberg, J.M., Gomez, G.A., Verma, S., Moussa, E.J., Wu, S.K., Priya, R., et al., (2014). Tension-sensitive actin assembly supports contractility at the epithelial zonula adherens. *Curr. Biol.* **24**, 1689–1699.
59. Hu, S.H., Dasbiswas, K., Guo, Z., Tee, Y.H., Thiagaragjan, V., Hersen, P., et al., (2017). Long-range self-organization of cytoskeletal myosin II filament stacks. *Nature Cell Biol.* **19**, 133–141.
60. Li, Y., Merkel, C.D., Zeng, X., Heier, J.A., Cantrell, P.S., Sun, M., et al., (2019). The N-cadherin interactome in primary cardiomyocytes as defined using quantitative proximity proteomics. *J. Cell Sci.* **132**, jcs221606.
61. Morris, T., Sue, E., Geniesse, C., Brieher, W.M., Tang, V. W., (2020). Synaptopodin is required for stess fiber and contractomere assembly at the epithelial junction. *bioRXiv*.
62. Hoelzle, M.K., Svitkina, T., (2012). The cytoskeletal mechanisms of cell-cell junction formation in endothelial cells. *Mol. Biol. Cell* **23**, 310–323.
63. Millan, J., Cain, R.J., Reglero-Real, N., Bigarella, C., Marcos-Ramiro, B., Fernandez-Martin, L., et al., (2010). Adherens junctions connect stress fibres between adjacent endothelial cells. *BMC Biol.* **8**, 11.
64. Owen, L.M., Bax, N.A., Weis, W.I., Dunn, A.R., (2022). The C-terminal actin binding domain of talin forms an asymmetric catch bond with F-actin. *Proc. Natl. Acad. Sci. U. S. A.* **119**, e2109329119
65. Yamada, S., Pokutta, S., Drees, F., Weis, W.I., Nelson, W. J., (2005). Deconstructing the cadherin-catenin-actin complex. *Cell* **123**, 889–901.
66. Miller, P.W., Pokutta, S., Ghosh, A., Almo, S.C., Weis, W. I., Nelson, W.J., et al., (2013). *Danio rerio* αE-catenin is a monomeric F-actin binding protein with distinct properties from *Mus musculus* αE-catenin. *J. Biol. Chem.* **288**, 22324–22332.
67. Pokutta, S., Weis, W.I., (2000). Structure of the dimerization and β-catenin binding region of α-catenin. *Mol. Cell* **5**, 533–543.
68. Rangarajan, E.S., Izard, T., (2013). Dimer asymmetry defines α-catenin interactions. *Nature Struct. Mol. Biol.* **20**, 188–193.
69. Shibahara, T., Hirano, Y., Hakoshima, T., (2015). Structure of the free form of the N-terminal VH1 domain of monomeric α-catenin. *FEBS Lett.* **589**, 1754–1760.